CMTM4 promotes the motility of colon cancer cells under radiation and is associated with an unfavorable neoadjuvant chemoradiotherapy response and patient survival in rectal cancer

LUJING YANG[1*], ZHITING MIAO[2*], NINGNING LI[2], LIN MENG[3], QIN FENG[2], DONGBO QIAO[2], PING WANG[2], YUE WANG[2], YANHUA BAI[2], ZHONGWU LI[2**] and SHENYI LIAN[2**]

[1]Department of Pathology, Beijing Friendship Hospital, Capital Medical University, Beijing 100050, P.R. China; [2]Department of Pathology, Key Laboratory of Carcinogenesis and Translational Research (Ministry of Education/Beijing), Peking University Cancer Hospital and Institute, Beijing 100142, P.R. China; [3]Department of Biochemistry and Molecular Biology, Key Laboratory of Carcinogenesis and Translational Research (Ministry of Education/Beijing), Peking University Cancer Hospital and Institute, Beijing 100142, P.R. China

Received June 18, 2024; Accepted December 2, 2024

DOI: 10.3892/ol.2025.14884

Abstract. Neoadjuvant chemoradiotherapy (nCRT) is the standard treatment for locally advanced rectal cancer (LARC). Pathological complete regression is closely linked to disease outcomes. However, biomarkers predicting nCRT response and patient survival are lacking for LARC. In the present study, the clinical characteristics and follow-up information of 228 patients with LARC were retrospectively collected. Immunohistochemistry (IHC), reverse transcription-quantitative PCR (RT-qPCR), Kaplan-Meier and multivariate analyses were used to evaluate the expression and predict the role of CKLF-like MARVEL transmembrane domain member 4 (CMTM4) in LARC. Additionally, lentiviral short hairpin (sh)RNA was used to interfere with CMTM4 expression. The phenotype of CMTM4-knockdown LoVo cells was determined by colony formation, migration and invasion assays under irradiation (IR) treatment. RNA-sequencing (RNA-seq) analysis was also used to explore the CMTM4-regulated genes in LoVo-shCMTM4 cells compared with control cells. RT-qPCR was then used to confirm the expression of these CMTM4-regulated genes. CMTM4 expression in pre-nCRT tissues indicated an unfavorable response and a short disease-free survival (DFS) with LARC. The expression of CMTM4 significantly increased following nCRT treatment. Additionally, CMTM4 knockdown increased the proliferation, migration and invasion of colon cancer cells; however, IR disrupted the cell migration and invasion induced by CMTM4 knockdown. RNA-seq analysis, the Tumor Immune Estimation Resource database and RT-qPCR indicated that CMTM4 was involved in different signaling pathways and regulated immune-related genes such as cluster of differentiation 66b, chemokine (CXC motif) ligand 8 (CXCL8) and programmed cell death 1. Furthermore, CXCL8 expression was found to be negatively associated with CMTM4 expression in patients with LARC by IHC and RT-qPCR. CXCL8 expression on invasion margin regions in post-operative tissues was also an inferior predictor of DFS in patients with LARC. In conclusion, CMTM4 may predict the nCRT response and outcomes in patients with LARC.

Correspondence to: Professor Zhongwu Li or Professor Shenyi Lian, Department of Pathology, Key Laboratory of Carcinogenesis and Translational Research (Ministry of Education/Beijing), Peking University Cancer Hospital and Institute, 52 Fucheng Road, Haidian, Beijing 100142, P.R. China
E-mail: zhwuli@hotmail.com
E-mail: liansypku@163.com

*, **Contributed equally

Abbreviations: LARC, locally advanced rectal cancer; nCRT, neoadjuvant chemoradiotherapy; pCR, pathological complete response; CRC, colorectal cancer; TME, total mesorectal excision; TNT, total neoadjuvant therapy; CR, complete response; CMTM, CKLF-like MARVEL transmembrane domain member; RT-qPCR, reverse transcription-quantitative qPCR; OS, overall survival; DFS, disease-free survival; READ, rectum adenocarcinoma; COAD, colon adenocarcinoma; TAMs, tumor-associated macrophages; Th, T helper, Tfh, Follicular helper T cell; ICI, immune checkpoints inhibitors; MRI, magnetic resonance imaging; CXCL8, chemokine (CXC motif) ligand 8

Key words: CMTM4, LARC, nCRT, CXCL8

Introduction

Colorectal cancer (CRC) ranks third in incidence and second in mortality of all cancer types worldwide (1). The incidence of CRC in the whole population of China has gradually increased in recent years (2). Some early stage CRC cases are suitable for endoscopic treatment; however, surgery is the primary and cornerstone treatment for curative purposes. Rectal cancer is more complex due to the intricate anatomy of the pelvis (3). Total mesorectal excision (TME) is the standard

approach for treating rectal cancer. Furthermore, neoadjuvant radiotherapy followed by TME and adjuvant chemotherapy is the standard treatment for locally advanced rectal cancer (LARC; staging, T3-4/N+M0). The combined treatment has led to a marked reduction in the rate of local recurrence in the past 10 years (4,5). Tumor downsizing and pathological complete response (CR) following neoadjuvant chemoradiotherapy (nCRT) has been observed in 15-20% of patients with LARC (4). However, no survival benefits were observed in patients with rectal cancer treated with preoperative radiation following TME by several long-term follow-up analyses (5-7). Therefore, exploring an alternative approach or identifying an nCRT response or survival predictor is necessary and urgent. It has been reported that total neoadjuvant therapy (TNT) could increase the CR rate to 30% and improve life quality by anus preservation. nCRT combined with immunotherapy is also a promising approach for treating patients with rectal cancer (5). Regardless of whether nCRT, TNT or combined immunotherapy is used, a biomarker that can predict radiation response before or after nCRT remains necessary.

CKLF-like MARVEL transmembrane domain member 4 (CMTM4) is a member of the chemokine-like factor (CKLF) superfamily, of which there are 9 members: CKLF and CMTM 1-8. The MARVEL domain in CMTM4 is responsible for vesical trafficking and membrane linking (8). To date, the expression of CMTM4 has been found to be lower in tumor tissues compared with adjacent normal tissues in CRC and clear cell renal carcinoma (9,10). CMTM4 serves as a tumor suppressor and has been shown to inhibit cell proliferation and migration through the AKT, ERK1/2 and signal transducer and activator of transcription (STAT) 3 pathways in CRC cell lines (9.10). It has also been demonstrated that CMTM4 is upregulated in human head and neck squamous cell carcinoma (HNSCC) and indicates poorer survival and lymphatic metastasis by regulating epithelial-mesenchymal transition (EMT) and programmed death ligand 1 (PDL1) expression (11). The expression and prognostic role of CMTM4 in hepatocellular carcinoma (HCC) proposed by several groups from previous studies has been contradictory. Chui *et al* (12) and Zhou *et al* (13) reported that upregulation of CMTM4 in patients with HCC was related to poor survival. Studies from Tan *et al* (14) and Bei *et al* (15) reported that high expression of CMTM4 was associated with a good survival in patients with HCC. Studies have shown that CMTM4/6 stabilizes PDL1 expression by inhibiting protease or lysosome-mediated degradation (16,17). Therefore, targeting the CMTM4/6-PDL1 pathway could be a new avenue to enhance antitumor effectiveness of current PD-L1/PD-1 blocking therapies. CMTM6, which shares 55% sequence homology with CMTM4, has been reported to be involved in immunosuppressive microenvironments in glioma, renal carcinoma and CRC (18). Data from The Cancer Genome Atlas (TCGA) database showed that CMTM4 expression is negatively correlated with cytotoxic, dendritic, T and $CD8^+$ T cells (13,14). The immune-related function of CMTM4 has rarely been reported. Furthermore, the role of CMTM4 in rectal cancer, particularly in LARC treated with nCRT, remains unclear.

In the present study, 228 patients with LARC were retrospectively enrolled, including 178 with paired pre-/post-operative tissues and 50 pathological complete response (pCR) patients with preoperative tissues. The aim of the present study was to reveal the predictive role of CMTM4 in patients with LARC and its underlying biological mechanism in LARC and colon cancer.

Materials and methods

Patient selection. Data were retrospectively collected from 228 patients with LARC who received intensity-modulated radiation therapy (IMRT) with concurrent capecitabine treatment followed by surgery at Peking University Cancer Hospital (Beijing, China) between December 2008 and June 2015. The IMRT regimen consisted of 22 fractions of 2.3 Gy (gross tumor volume) and 1.9 Gy (clinical target volume), which has been described previously (19). Surgery was recommended ≥8 weeks after the completion of radiation. Adjuvant chemotherapy was also routinely recommended to the patients. Each enrolled patient satisfied the following criteria: i) Cancerous lesion located within 10 cm from the anal verge; ii) cancer staged as T3-4 or any T and N+ by endorectal ultrasonography (7th AJCC cancer staging system) (20), pelvic magnetic resonance imaging (MRI) or computed tomography; iii) presence of distant metastases excluded by imaging examinations; iv) preoperative radiotherapy of 50.6 Gy/22 fractions; and v) radical surgery following TME. Patients with the following characteristics were excluded from the present study: i) Previous chemotherapy or pelvic radiation; ii) previous history (within 5 years) of malignant tumor; and iii) presence of unresectable cancer. All patients signed the consent forms before treatment. The patient information and samples were gathered from the hospital surgical database. The blocks of formalin-fixed paraffin-embedded (FFPE) samples from each patient in this surgical database were stored at The Department of Pathology at Peking University Cancer Hospital. The slices of FFPE samples were stored at -80˚C for long term and -20˚C for short term storage. The present retrospective study was approved by The Ethics Committee of Peking University Cancer Hospital (approval no. 2021KT93). Informed consent for inclusion in the present study was waived by The Ethics Committee due to the retrospective nature of the present study.

Immunohistochemistry (IHC). FFPE tissue sections (5 μM) were prepared and stained with hematoxylin (5 min) and eosin (2 min) at room temperature for histological evaluation. For IHC, the sections were deparaffinized in a xylene and an ethanol gradient at room temperature. Antigen retrieval was performed with citrate buffer pH 6.0 at 95˚C for 10 min, followed by incubating with an endogenous peroxidase blocker (cat. no. ZLI-9310; ZSGB-Bio) for 10 min at room temperature. The sections were then washed with PBST (0.1% Tween-20) for 5 min three times and incubated with 5% goat serum (cat. no. ZLI-9021; ZSGB-Bio) for 1 h at room temperature. The sections were incubated with the following primary antibodies at 4˚C overnight: chemokine (CXC motif) ligand 8 (CXCL8; 1:500; cat. no. 27095-1-AP; Proteintech Group, Inc.) and CMTM4 (1:500; cat. no. HPA014704; Sigma-Aldrich; Merck KGaA). Following washing with PBST (0.1% Tween-20) three times, the slices were incubated with the secondary antibody (undiluted; cat. no. SAP-9100; ZSGB-Bio) at room temperature for 40 min. Diaminobenzidine (Dako; Agilent

Technologies, Inc) substrate was used to observe staining, and the sections were re-stained with hematoxylin for 5 min at room temperature (Beyotime Institute of Biotechnology). A bright field microscope (Leica Microsystems, Inc.) was used to capture images. The H score is a reliable method that can effectively quantify protein expression by two independent pathologists (21). The H score was calculated as follows: (Percentage of weak staining) + (Percentage of moderate staining) + (Percentage of strong staining) within the target region, with scores ranging from 0 to 300 (22). The of CMTM4 and CXCL8 had different expression pattern, therefore the cut-off value is different. H scores of 0-120 were defined as the CXCL8 low group and H scores of 121-300 as the CMTM4 high group. H scores of 0-150 were defined as the CMTM4 low group and H scores of 151-300 as the CXCL8 high group.

Cell culture. The human colon cancer LoVo cell line purchased from the American Type Culture Collection (cat. no. CCL-229) was cultured in a hot cell incubator (5% CO_2, 37˚C) in RPMI-1640 (Invitrogen; Thermo Fisher Scientific, Inc.) supplemented with 10% bovine serum (cat. no. 164210; Procell Life Science & Technology Co., Ltd.) and 100 U/ml streptomycin. When the cells reached 80-90% confluency, pancreatin digestion was carried out and the cells were resuspended in fresh culture medium. The consumables used for cell culture were sterilized by high pressure and the cells were regularly examined for mycoplasma contamination by reverse transcription-quantitative PCR (RT-qPCR).

Cell transfections. The lentivirus targeting human CMTM4 and an shRNA scramble sequence (negative control; NC) were generated and synthesized by GenePharma Co., Ltd. The short hairpin (sh)RNAs used in the present study were as follows: shCM4-3, GAAAUUGCUGCCGUGAUAUTT; shCM4-6, GCAUAUGCAGUGAACACAUTT; and sh NC, UUCUCC GAACGUGUCACGUTT. Briefly, the shRNAs targeting human CMTM4 were cloned into a 3rd generation lentiviral transfer plasmid, pLV-eGFP (vector backbone, pLenti-MP2), generating a lenti-shCMTM4 construct for expression knockdown. The virus was added at a volume ratio of 1:100 and at a titer of $1x10^8$ TU/ml into LoVo cells, while simultaneously adding polybrene at a volume ratio of 1:500 at 37˚C and 5% CO_2. Fresh and complete culture medium was replaced within 24 h from infection, and the infection efficiency was detected using western blotting and immunofluorescence after 72 h.

Adenovirus carrying the human CMTM4 gene and the empty adenovirus were packaged by GenePharma Co., Ltd. LoVo cells were infected with the adenovirus at a multiplicity of infection of 100 for 72 h. All other steps were as described above.

Irradiation. The LoVo cells were infected with the indicated lentivirus for 72 h before irradiation. X-ray irradiation was performed using an X-ray generator (EDGE™ Radiosurgery system; Varian Medical Systems, Inc.) with gantry 0˚, collimator 0˚, field 30x30 cm, energy 6 Mv with extra-fine 2.5 mm MLC leaves. Indicated doses were shown in each experiment.

Western blotting. A total of $2x10^6$ cells with the indicated treatments were harvested and lysed using RIPA buffer containing 50 mM Tris-HCl pH 7.4, 150 mM NaCl, 50 mM NaF, 1 mM EDTA, 1 mM DTT, 1% TritonX-100, 0.1% sodium dodecyl sulphate (SDS) and 1X protease inhibitor cocktail. After a 20-min incubation on ice, the cell lysates were centrifuged at 13,800 x g for 20 min at 4˚C, and the supernatants were recovered. Protein samples (20 μg) were resolved by 12% SDS-polyacrylamide gel electrophoresis and blotted onto polyvinylidene fluoride membrane (cat. no. 88520; Thermo Fisher Scientific, Inc.), which was blocked in 5% skim milk in TBST (Tris-buffered saline containing 0.1% Tween-20) at room temperature for 45 min. The membrane was then probed with rabbit anti-CMTM4 (1:500; cat. no. HPA014704; Sigma-Aldrich; Merck KGaA) and mouse anti-GAPDH (1:1,000; cat. no. TA-082519; OriGene Technologies, Inc.) antibodies overnight at 4˚C. Following washing with TBST, the membrane was incubated with the HRP-anti-mouse (1:2,000; cat. no. ab6789; Abcam), HRP-anti-rabbit (1:2,000; cat. no. ab6721; Abcam) secondary antibody at room temperature for 45 min. The band strips were visualized using enhanced chemiluminescence detection system (cat. no. 34580; Thermo Fisher Scientific, Inc). and the images were captured using chemiluminescence imaging systems (Azure Biosystems, Inc.).

Colony formation assay. The cells were digested and counted, and 800 cells from each group were resuspended in fresh culture medium. After 10-14 days of cell culture, the cells were fixed at room temperature with precooled methanol for 30 min, the methanol was discarded, the cells were washed with PBS three times and then incubated with 1% crystal violet dye solution for 30 min at room temperature. The cells were then washed with PBS three times and dried in a fume hood. The bottom of the cell plate was scanned, and the number of clusters with >50 cells were counted using ImageJ software (National Institutes of Health; V48.1).

Transwell assay. Migration (cat. no. 3422; Corning, Inc.) and invasion assays (cat. no. 354480; Corning, Inc.) were performed using 8-μm pore size plates with a filter insert. The invasion inserts precoated with diluted Matrigel, were preheated at 37˚C for 1 h before the invasion experiments. Briefly, $2x10^5$ cells resuspended in 200 μl medium without serum were inoculated into the upper chamber of each well; 800 μl medium containing 10% FBS was then added to the lower chamber. The cells were allowed to migrate for 36-48 h at 37˚C. The rotating pores were fixed in 100% methanol and dyed in 0.1% crystal violet solution at room temperature for 30 min. The cells in the upper chamber were then removed with absorbent cotton. The polycarbonate membrane was then removed and sealed on a glass slide with resin, and the cells penetrating the underside of the membrane were counted in four randomly selected visual fields.

Tumor immune Estimation Resource (TIMER) database analysis. The TIMER database (https://cistrome.shinyapps.io/timer) is a comprehensive online analysis software for investigating the gene expression and immune cell infiltration in different cancer types (23). The TIMER database contains 166 rectum adenocarcinoma (READ) tumor samples and 10 normal samples; 457 colon adenocarcinoma (COAD) tumor samples and 41 normal samples. TIMER was used to explore

the correlation between CMTM4 and the levels of immune cell infiltration. The association of CMTM4 expression with gene marker of different immune cell including $CD4^+$ T cells, $CD8^+$ T cells, B cells, macrophages, neutrophils and monocytes were further investigated (24). P≤0.05 was considered to indicate a statistically significant difference.

Microarray analysis and Kyoto Encyclopedia of Genomics and Genomics (KEGG) enrichment analysis. To use high-throughput methods to analyze gene expression patterns under different experimental conditions, microarray analysis was performed. Total RNA was extracted from the indicated samples using Qiagen RNeasy kit (cat. no. 74104; Qiagen GmbH). The mRNA library construction and RNA-seq analysis were constructed and performed by Shenzhen BGI Co., Ltd. using the Illumina Genome Analyzer platform. The differentially expresses genes with false discovery rate<0.01, fold change >1.5 were determined. Principal component analysis was performed using the 'stats' package and plotted with the 'ggplot2' package in R (version 3.5) (25). Gene Set Enrichment Analysis (GSEA) was performed using the GSEA software (Broad Institute) as previously described (26). DAVID analysis was performed for transcription factor enrichment as previously described (27,28).

RT-qPCR. Total RNA was extracted from cell lines and FFPE tissues using TRIzol® reagent (cat. no. 10057821; Thermo Fisher Scientific, Inc.) and RNeasy FFPE Kit (cat. no. 73504; Qiagen GmbH), respectively, according to the manufacturer's instructions. cDNA was synthesized using a GoScript™ reverse transcription system (cat. no. A5001; Promega Corporation) according to the manufacturer's instructions. Each assay was tested in duplicate. The expression of CMTM4 and CXCL8 were assessed by SYBR GREEN Mixture (ROX reference dye; cat. no. QPK-201; Toyobo Co., Ltd.). For the RT-qPCR experiments of cell lines and FFPE, GAPDH served as the internal control. Relative mRNA expression was calculated using $2^{-\Delta\Delta Cq}$ (29). The thermocycling conditions were as follows: Pre-denatured at 95˚C for 5 min, 40 cycles at 95˚C for 10 sec, 60˚C for 20 sec and 72˚C for 20 sec. The primers used are listed in Table SI.

Statistical analysis. Data was analyzed using GraphPad Prism 8.3 (Dotmatics) and SPSS 25 (IBM Corp.). Comparison of multiple groups was performed using one-way ANOVA and Tukey's post hoc test. Comparisons of CMTM4 or CXCL8 expression from pre-operative with post-operative tissues were performed using paired t-test. Comparison of the RT-qPCR results between the CMTM4 control and overexpression/shRNA groups was performed using unpaired t-test. The results are presented as the mean ± standard deviation from at least three independent experiments. The optimal cut-off value and Kaplan-Meier curves of CMTM4 and CXCL8 in the survival analysis were determined with the 'survival' (R version 3.7.0) and 'survminer' package (R version 4.3.2; http://www.R-project.org). Following cut-off value determination, patients were stratified into high- and low-expression groups for each biomarker. Disease-free survival (DFS) and overall survival (OS) were evaluated using Kaplan-Meier curves to illustrate differences in survival distributions, with group comparisons performed via the log-rank test. The univariable and multivariable Cox proportional hazards regression models were applied to assess the prognostic significance of CMTM4, adjusting for relevant clinical covariates where appropriate. For all statistical tests, including the log-rank comparisons and Cox regression analyses, a single-sided P<0.05 was considered to indicate a statistically significant difference.

Results

CMTM4 expression indicates radiotherapy resistance in rectal cancer. In total, 228 consecutive patients with rectal cancer (152 men and 76 women) were included in the present study. The median age of the patients was 57 years (range, 25-80 years), the median follow-up time was 54.7 months and 73 (32.0%) patients experienced recurrence or metastasis. Overall, 21.8% of patients reached pathological complete response [pCR; no observed adenocarcinoma cells in the surgical resection specimen, pathological stage after nCRT (yp) T0N0M0 (30)] following nCRT. Downstaging (ypT0-2N0M0) occurred in 134 patients (58.8%). Additional post-operative characteristics and distribution of relevant parameters are listed in Table I. Patients with pN+, pT3 or nerve invasion were significantly associated with a poorer overall survival (OS; P=0.001, P=0.042 and P<0.001, respectively) and DFS (P<0.001, P=0.001 and P=0.008, respectively) (Table II).

CMTM4 staining was conducted on pre- and post-operative tissues from patients with LARC. CMTM4 was localized in the cell membrane and cytoplasm in patients with LARC and chemoradiotherapy did not change the CMTM4 localization (Fig. 1A). To confirm the IHC observations, five samples with high and three with low CMTM4 expression were selected for analysis, and DNA was extracted from these samples. The average relative level of CMTM4 in the IHC high group was 1.477 and in the IHC low group was 0.487 (P=0.015; Fig. 1B). The results of the RT-qPCR experiments indicated that the protein expression detected by IHC was consistent with the mRNA expression level. Therefore, the expression detected by IHC was reliable in the downstream analysis. CMTM4 exhibited lower expression in tumor tissues compared with adjacent normal tissues in the postoperative samples (P<0.0001; Fig. S1A). Lower CMTM4 expression in pre-operative tissues was significantly associated with improved DFS and OS (P=0.029 and P=0.048, respectively; Fig. 1C). CMTM4 expression in LARC tissues following TME surgery was not associated with OS or DFS (P=0.18 and P=0.168, respectively; Fig. S1B). The multivariate model was employed to evaluate the comprehensive prognostic value of features obtained from the univariate analysis. CMTM4 was an independent prognostic factor of DFS [hazard ratio (HR), 1.759; 95% confidence interval (CI), 1.037-2.984; P=0.036] in patients with LARC and nerve invasion and pN+ in post-nCRT was an independent prognostic factor of OS and DFS in patients with LARC (Table III). The changes in CMTM4 expression were compared between pre-nCRT and post-nCRT and radiation therapy significantly increased CMTM4 expression (P=0.031; Fig. 1D). Further analysis indicated that CMTM4 expression in the pCR group was lower than that in the non-pCR groups (P=0.041; Fig. 1E). In summary, CMTM4, a potential new biomarker for patients with LARC before nCRT,

Table I. Distribution of relevant parameters after nCRT.

Variables	No. of patients	% of patients
Age, years		
≤58	114	50.0
>58	114	50.0
Sex		
Male	152	66.7
Female	76	33.3
TRG		
0	50	21.9
1	61	26.8
2	103	45.2
3	14	6.1
pCR		
Yes	50	21.9
No	178	78.1
Down staging (pT-cT)		
Yes	134	58.8
No	94	41.2
Lymph node sampling		
≥8	103	45.2
<8	125	54.8
Vascular invasion		
Yes	6	2.6
No	222	97.4
Nerve invasion		
Yes	4	1.8
No	224	98.2
Clinical T stage		
2	28	12.3
3	172	75.4
4	28	12.3
Pathological T stage		
ypT0	50	21.9
ypT1	14	5.7
ypT2	63	28.5
ypT3	101	43.9
Pathological N stage		
ypN0	188	82.5
ypN+	40	17.5
Tumor deposit		
Yes	15	6.6
No	213	93.4
MMR status		
pMMR	202	88.6
dMMR	26	11.4

TRG, tumor regression grading; pCR, pathologic complete response; MMR, mismatch repair; pMMR, mismatch repair proficient; dMMR, mismatch repair deficient; pT, pathological T stage; cT, clinical T stage; nCRT, neoadjuvant chemoradiotherapy; T, tumor; N, node.

was negatively associated with chemoradiotherapy response and prognosis.

CMTM4 knockdown impaired cell migration and invasion triggered by radiation. To further investigate the role of CMTM4 in chemoradiotherapy, a CMTM4 knockdown cell line was established using lentivirus shRNA. The knockdown efficiency was verified by immunofluorescence, western blotting and RT-qPCR (Fig. 2A-C). Compared with the NC cells, CMTM4 knockdown significantly increased cell proliferation, migration and invasion (Fig. 2D-F). Following radiation exposure (2 and 5 Gy), there was no significant difference between the NC and CMTM4 knockdown groups in terms of colony formation ability (Fig. 2D). However, compared with the NC group, interfering with CMTM4 knockdown significantly decreased the cell migration and invasion under IR treatment (Fig. 2E and F). These *in vitro* experiments were consistent with the findings in the clinical data; CMTM4 expression induced radiotherapy resistance in colon cancer cells.

CMTM4 participates in multiple pathways in colon cancer and regulates the expression of immune-related cytokines. RNA samples were extracted from LoVo-NC, LoVo-shCM4-3 and LoVo-shCM4-6 cells, and microarray analysis was performed to examine the effect of CMTM4 on the gene expression profiles (Fig. 3A). Compared with the LoVo-NC group, the LoVo-shCM4-3 group had 184 upregulated and 220 downregulated genes, while the LoVo-shCM4-6 group had 232 upregulated and 455 downregulated genes (Fig. 3B). The expression of 105 genes was mutually altered by CMTM4 knockdown, including 38 upregulated and 67 downregulated genes. CXCL8 was shown to be upregulated by CMTM4 knockdown in the RNA-seq analysis (Fig. 3C and Table SII). Gene ontology function analysis indicated that CMTM4 knockdown altered different pathways involved in 'Metabolism', 'Genetic Information Processing', 'Environmental Information Processing', 'Cellular Processes', 'Organismal Systems and 'Human Diseases' (Fig. 3D). These 105 genes were shown to participate in the KEGG pathways associated with different physiological and pathological processes including 'Metabolism', 'Genetic Information Processing', 'Cellular Processes' and 'Human Diseases'. The profiles of the representative top 19 KEGG enrichment pathways ($P<0.05$) are listed in Table SIII, such as 'Aminoacyl-tRNA biosynthesis' in translation, 'FoxO signaling pathway', 'PI3K-Akt signaling pathway' in signal transduction, 'Mitophagy' in transport and catabolism, 'Apoptosis' in cell growth and death, 'NOD-like receptor signaling pathway' in immune system.

nCRT typically triggers metabolism, inflammation and an immune system response (31,32). Therefore, the TIMER database was used to explore the association between CMTM4 and immune cell infiltration in READ. In the READ dataset, a significant although weak correlation was observed between CMTM4 expression and immune cell infiltration in B cells ($\rho=0.231$, $P=6.13\times10^{-03}$), $CD8^+$ T cells ($\rho=0.214$, $P=1.13\times10^{-02}$) but not with purity ($\rho=-0.105$, $P=2.16\times10^{-01}$), $CD4^+$ T cells ($\rho=0.033$, $P=7.03\times10^{-01}$), macrophages ($\rho=0.071$, $P=4.09\times10^{-01}$), neutrophils ($\rho=0.064$, $P=4.57\times10^{-01}$) and dendritic cells ($\rho=0.056$, $P=5.15\times10^{-01}$) (Fig. S2). The TIMER database was also used to further

Table II. Univariate analysis to identify prognosis-related factors.

Variable	No. of patients	OS, %	HR (95% CI)	P-value	DFS, %	HR (95% CI)	P-value
Age, years				0.594			0.809
≤58	114	75.4	1		66.7	1	
>58	114	79.8	0.860 (0.495-1.496)		68.4	0.945 (0.599-1.492)	
Sex				0.694			0.890
Male	152	77.0	1		67.1	1	
Female	77	78.9	0.888 (0.491-1.605)		68.4	0.966 (0.594-1.572)	
pCR				0.058			0.004
Yes	50	88.0	1		86.0	1	
No	178	74.7	2.282 (0.973-5.350)		62.4	3.171 (1.455-6.912)	
Vascular invasion				0.730			0.954
Yes	6	83.3	1		66.7	1	
No	222	77.5	0.706 (0.097-5.111)		67.6	0.959 (0.235-3.910)	
Nerve invasion				<0.001			0.008
Yes	4	25.0	1		25.0	1	
No	224	78.6	0.119 (0.036-0.390)		68.3	0.206 (0.064-0.657)	
Pathological T stage				0.042			0.001
ypT0	50	88.0	1		86.0	1	
ypT1	14	69.2	2.773 (0.782-9.783)		76.9	1.756 (0.454-6.795)	
ypT2	63	84.6	1.362 (0.495-3.750)		73.8	2.092 (0.867-5.045)	
ypT3	101	69.0	2.837 (1.183-6.803)		53.0	4.177 (1.886-9.248)	
Pathological N stage				0.001			<0.001
ypN+	40	57.5	1		40.1	1	
ypN0	188	81.9	0.373 (0.212-0.656)		73.4	0.321 (0.197-0.525)	
CMTM4 (pre-nCRT)				0.131			0.025
Low	81	82.7	1		76.5	1	
High	147	74.8	1.607 (0.868-2.974)		62.6	1.820 (1.080-3.068)	

pCR, pathologic complete response; nCRT, neoadjuvant chemoradiotherapy; OS, overall survival; DFS, disease-free survival; HR, hazard ratio; CI, confidence interval; T, tumor; N, node.

evaluate the association between CMTM4 expression and immune marker sets in READ and colon adenocarcinoma (COAD). The association between CMTM4 and immune cell markers of B cells, monocytes, tumor-associated macrophages (TAMs), M1 macrophages, M2 macrophages, neutrophils, natural killer cells, dendritic cells, general T cells and $CD8^+$ T cells were examined. Potential CMTM4-related immune gene markers in READ were selected as follows: Cor>0.15 and P<0.05, which were found only in the READ dataset and not in COAD. As shown in Table IV, with or without tumor purity adjustment, negative weak correlations were observed between CMTM4 and IL-10 in TAMs (ρ=-0.229, P=2.97x10^{-03}; ρ=-0.21, P=1.30x10^{-02}), cluster of differentiation 33 (CD33; ρ=-0.186, P=1.66x10^{-02}; ρ=-0.180, P=3.41x10^{-02}) in neutrophils and transforming growth factor β1 in T follicular helper (Tfh) cells (ρ=-0.221, P=4.31x10^{-03}; ρ=-0.275, P=1.04x10^{-03}). Without tumor purity adjustment, CMTM4 expression was weakly negatively correlated with CXCL8 (ρ=-0.159, P=4.10x10^{-02}), IL13 in T helper (Th)2 (ρ=-0.186, P=1.64x10^{-02}) and granzyme B in exhausted T cells (GZMB; ρ=-0.158, P=4.15x10^{-02}). Taking tumor purity into consideration, CD66b in neutrophils (ρ=-0.257, P=2.27x10^{-03}) and programmed cell death 1 in T cell exhaustion (ρ=-0.172, P=4.24x10^{-02}) were negatively correlated with CMTM4 expression in READ. BDCA-4, otherwise known as neuropilin-1, (ρ=0.169, P=2.95x10^{-02}; ρ=0.271, P=1.24x10^{-03}) in dendritic cells, STAT1 in Th1 cells (ρ=0.178, P=2.15x10^{-02}; ρ=0.253, P=2.6x10^{-03}) and B-cell lymphoma 6 (ρ=0.191, P=1.36x10^{-02}; ρ=0.219, P=9.46x10^{-03}) were weakly positively correlated with CMTM4 expression in READ with or without tumor purity adjustment. Without tumor purity adjustment, CMTM4 expression was only weakly positively correlated with that of IL-21 (ρ=0.154; P=4.77x10^{-02}) in Tfh cells. The association between CMTM4 and other gene markers, as well as B cells, monocytes, TAMs, M1 macrophages, M2 macrophages, nature killer cells, dendritic cells and CD8 cells are shown in Table SIV. V-set and immunoglobulin domain containing 4 and membrane spanning 4-domains A4A in M2 macrophages, HLA-DPB1, HLA-DQB1, HLA-DRA and HLA-DPA1 in dendritic cells and CD3D in general T cells were related to CMTM4 expression in both COAD and READ. Meanwhile, STAT3 in T helper 17 and STAT5B in

Table III. Multivariate analysis to identify prognosis-related factors.

	OS		DFS	
Variable	HR (95% CI)	P-value	HR (95% CI)	P-value
Nerve invasion		0.012		0.041
Yes	1		1	
No	0.212 (0.064-0.709)		0.289 (0.088-0.953)	
pCR		0.412		0.006
Yes	1		1	
No	1.451 (0.596-3.534)		2.031 (0.904-4.564)	
Pathological N stage		0.002		<0.001
ypN0	1		1	
ypN+	2.681 (1.458-4.933)		2.709 (1.634-4.492)	
CMTM4 (pre-nCRT)				0.036
Low			1	
High			1.759 (1.037-2.984)	

pCR, pathologic complete response; HR, hazard ratio; CI, confidence interval; T, tumor; N, node.

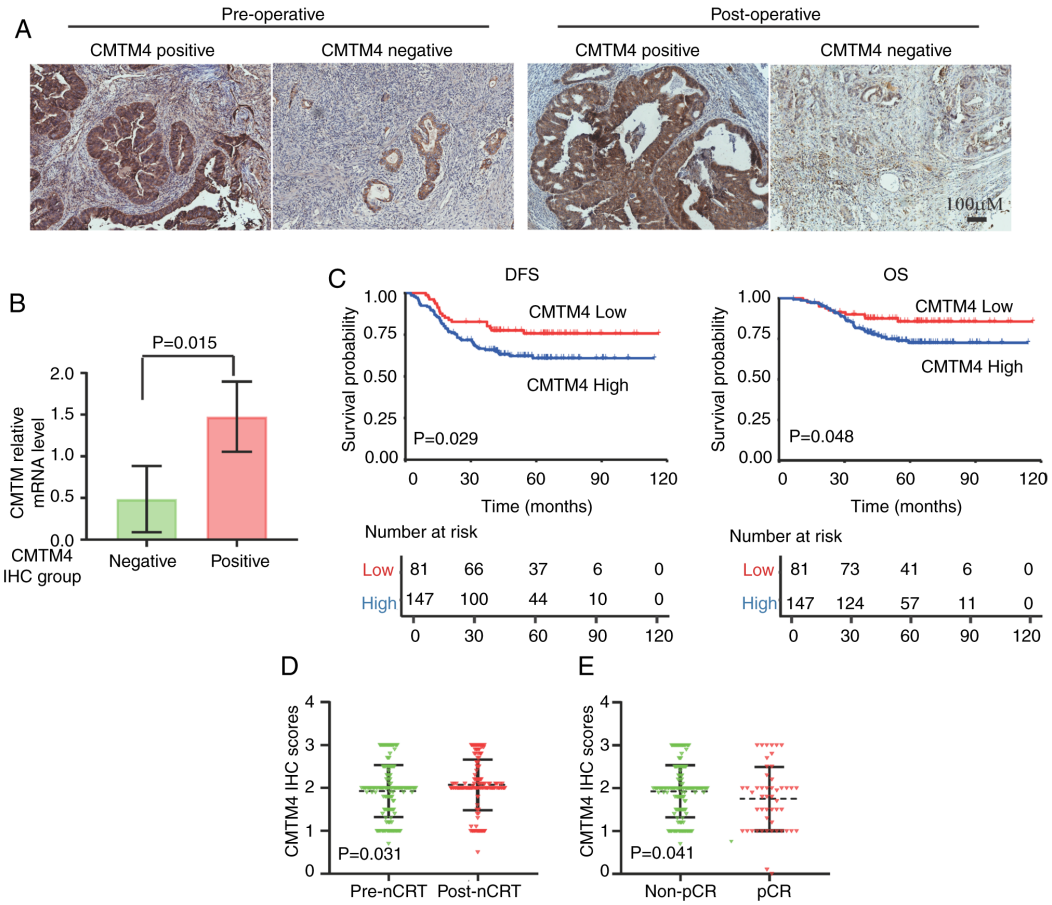

Figure 1. CMTM4 expression is linked to an unfavorable nCRT response in patients with LARC. (A) Representative IHC images of CMTM4 expression in pre- and post-operative tissues from patients with LARC. Scale bar, 100 μM. (B) The mRNA expression level of CMTM4 was higher in the IHC high group than in then IHC low group (P=0.015). DNA was extracted from 5 postoperative tissues with low CMTM4 expression and 3 tissues with low CMTM4 expression and amplified. (C) Kaplan-Meier survival curves of CMTM4 expression from pre-operative tissues in patients with LARC. CMTM4 was associated with a poorer DFS (P=0.029) and OS (P=0.048) in patients with LARC. (D) Changes in CMTM4 expression following nCRT in patients with LARC. nCRT increased CMTM4 expression in patients with LARC (P=0.031). (E) High CMTM4 expression in pre-operative tissues indicates unfavorable nCRT response. The expression of CMTM4 in pre-operative tissues was significantly lower in pCR patients than in non-pCR patients (P=0.041). CMTM4, CKLF-like MARVEL transmembrane domain member 4; LARC, locally advanced rectal cancer; nCRT, neoadjuvant chemoradiotherapy; IHC, immunohistochemistry; DFS, disease-free survival; OS, overall survival.

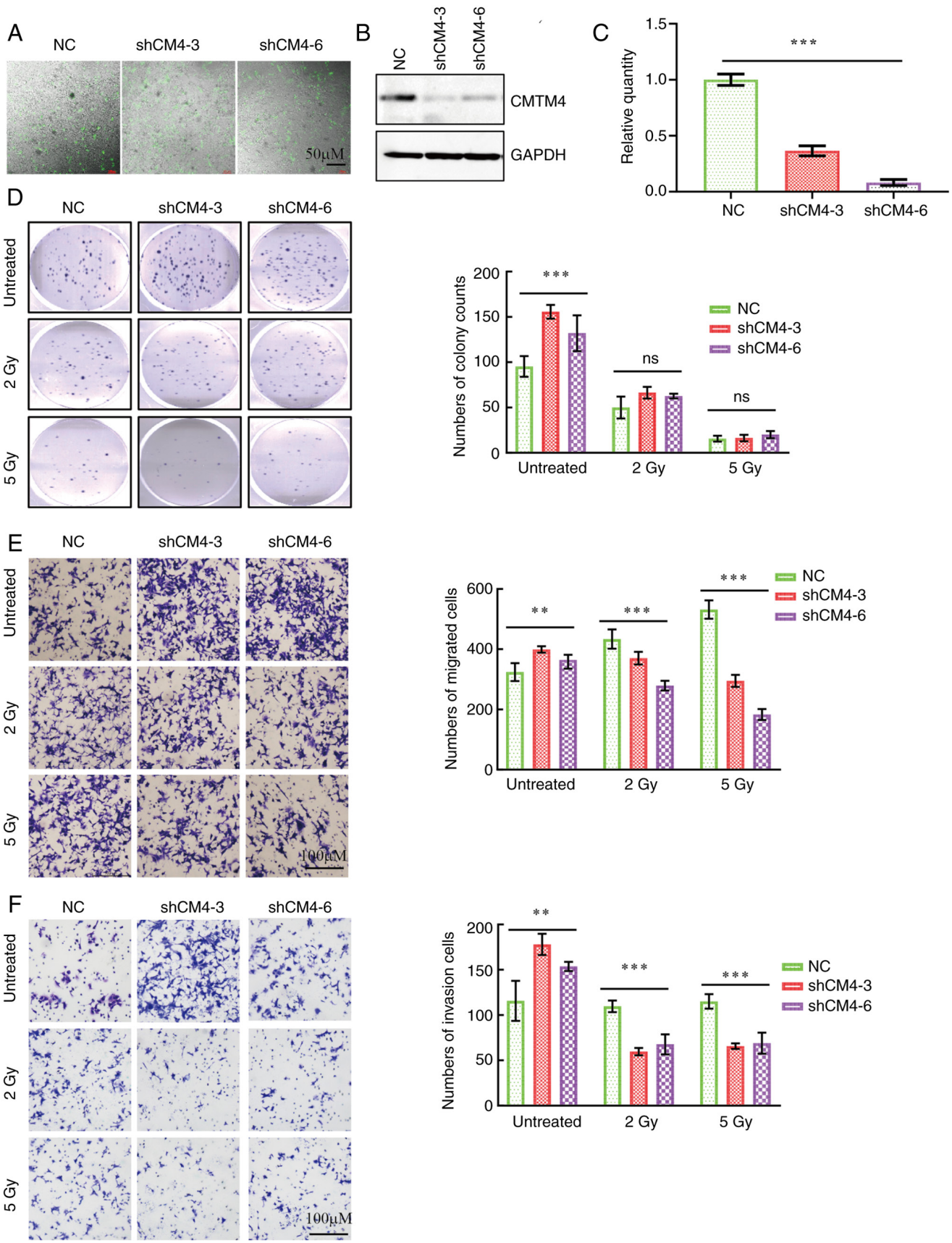

Figure 2. Radiation impairs cell proliferation, migration and invasion triggered by CMTM4 knockdown. (A) Representative immunofluorescence images of CMTM4 knockdown in LoVo cells. Scale bar, 50 μM. (B) Western blotting and (C) reverse transcription-quantitative PCR of CMTM4 expression in LoVo cells transfected with lenti-shCM4-3, lenti-shCM4-6 and NC. (D) IR impaired the cell proliferation induced by CMTM4 knockdown. Left panel, representative images of colony formations; right panel, quantification of cell count in colony formation experiments. IR inhibited the cell (E) migration and (F) invasion of lenti-shCMTM4 cells compared with the control cells. Left panel, representative images of cell migration and invasion; right panel, quantification of cell counts in Transwell experiments. Scale bar, 100 μM. Data are presented as the mean ± SEM from three independent experiments. **P<0.01 and ***P<0.001, determined by one-way ANOVA. ns, not significant. NC, negative control; CMTM4, CKLF-like MARVEL transmembrane domain member 4; IR, irradiation.

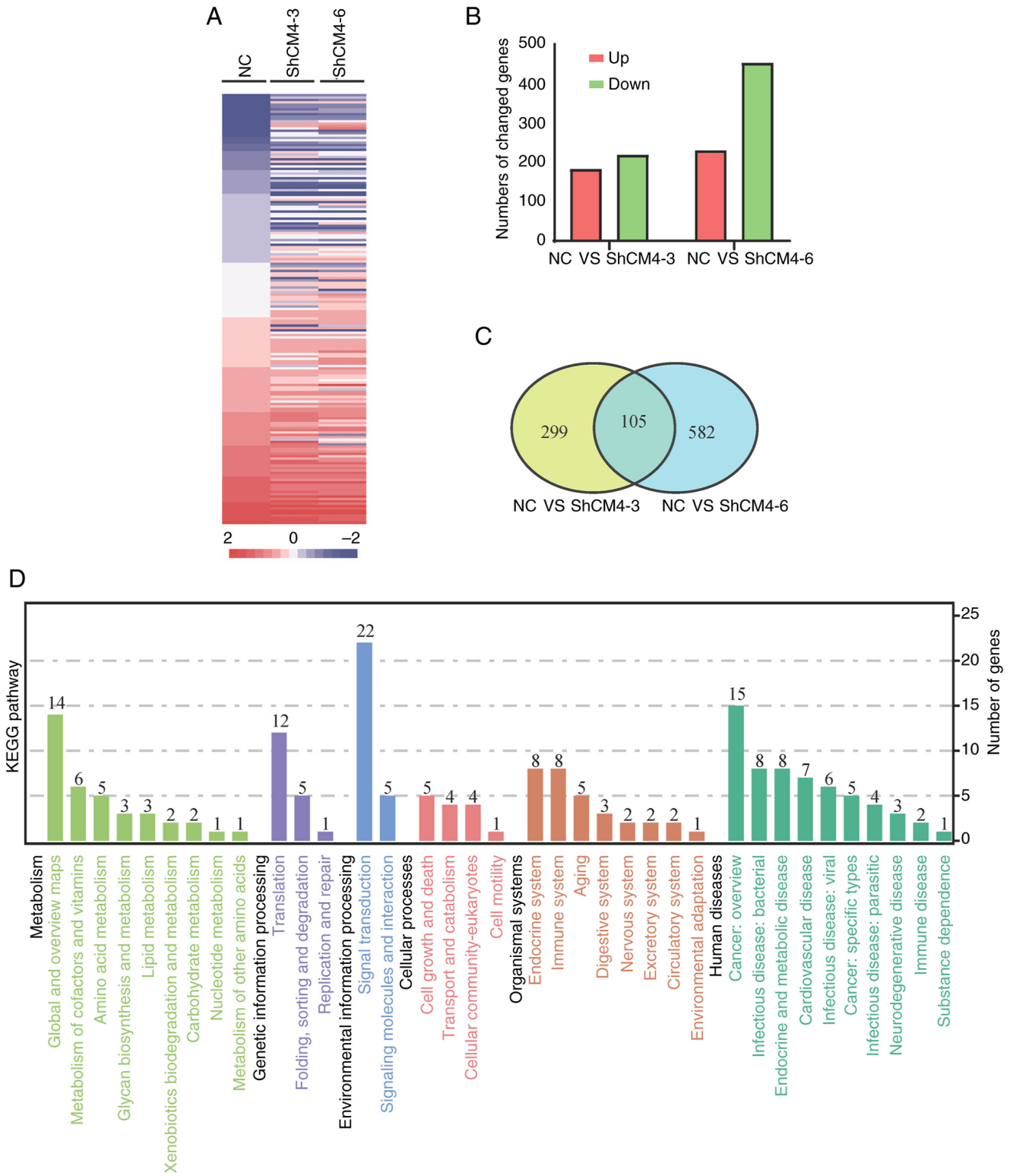

Figure 3. CMTM4 participates in multiple signal pathways. (A) Heatmap of genes regulated by decreased CMTM4 expression (shCM4-3 or shCM4-6 cells). Expression levels of upregulated and downregulated genes are represented in red or blue colors, respectively. (B) Numbers of altered genes in shCM4-3 and shCM4-6 cells, compared with NC cells. (C) Venn diagram of differentially expressed genes (FDR <0.01, fold change >1.5) in LoVo cell lines following CMTM4 knockdown (shCM4-3 and shCM4-6) compared with NC cells. Yellow circles indicate the numbers of genes up- or downregulated in the shCM4-3 group compared with the NC group; blue circles indicate the numbers of genes up- or downregulated in the shCMTM4-6 group compared with the NC group. In total, 105 genes were up- or downregulated following CMTM4 knockdown. (D) Altered genes from RNA-seq analysis were annotated by Gene Ontology Enrichment Analysis tools, indicating vital biological processes that were involved in LoVo cells following CMTM4 knockdown. CMTM4, CKLF-like MARVEL transmembrane domain member 4; FDR, false discovery rate; NC, negative control; sh, short hairpin RNA.

regulatory T cells were positively correlated with CMTM4 expression in both COAD and READ.

CXCL8 is negatively correlated with CMTM4 and indicates poor outcomes in patients with LARC. To verify the RNA-seq

Table IV. Correlation of CMTM4 and gene markers on immune cell infiltration.

		COAD				READ			
		None		Purity		None		Purity	
Cell type	Marker	Cor	P-value	Cor	P-value	Cor	P-value	Cor	P-value
TAM	IL10	-0.092	$5.02x10^{-02}$	-0.084	$8.99x10^{-2}$	-0.229	$2.97x10^{-03}$	-0.21	$1.30x10^{-02}$
Neutrophils	CD66b (CEACAM8)	0.016	$7.39x10^{-01}$	-0.027	$5.88x10^{-01}$	-0.134	$8.62x10^{-02}$	-0.257	$2.27x10^{-03}$
	CXCL8	-0.098	$3.63x10^{-02}$	-0.09	$6.97x10^{-02}$	-0.159	$4.10x10^{-02}$	-0.117	$1.71x10^{-01}$
	CD33	-0.136	$3.46x10^{-03}$	-0.132	$7.55x10^{-03}$	-0.186	$1.66x10^{-02}$	-0.18	$3.41x10^{-02}$
Dendritic cells	BDCA-4 (NRP1)	0.015	$7.54x10^{-01}$	0.032	$5.19x10^{-01}$	0.169	$2.95x10^{-02}$	0.271	$1.24x10^{-03}$
Th1	STAT1	0.002	$9.70x10^{-01}$	-0.107	$2.16x10^{-02}$	0.178	$2.15x10^{-02}$	0.253	$2.63x10^{-03}$
Th2	IL13	-0.076	$1.06x10^{-01}$	-0.058	$2.47x10^{-01}$	-0.186	$1.64x10^{-02}$	-0.142	$9.52x10^{-02}$
Tfh	BCL6	0.069	$1.40x10^{-01}$	0.085	$8.90x10^{-02}$	0.191	$1.36x10^{-02}$	0.219	$9.46x10^{-03}$
	IL21	-0.069	$1.39x10^{-01}$	-0.068	$1.74x10^{-01}$	0.154	$4.77x10^{-02}$	0.134	$1.17x10^{-01}$
Treg	TGFβ (TGFB1)	-0.131	$5.08x10^{-03}$	-0.122	$1.39x10^{-02}$	-0.221	$4.31x10^{-03}$	-0.275	$1.04x10^{-03}$
Exhausted T cells	PD-1 (PDCD1)	-0.12	$1.01x10^{-02}$	-0.109	$2.79x10^{-02}$	-0.130	$9.39x10^{-02}$	-0.172	$4.24x10^{-02}$
	GZMB	-0.086	$6.73x10^{-02}$	0.094	$5.92x10^{-02}$	-0.158	$4.15x10^{-02}$	-0.131	$1.23x10^{-01}$

COAD, colon adenocarcinoma; READ, rectum adenocarcinoma; IL10, Interleukin-10; CD66b (CEACAM8), Cluster of Differentiation 66b (Carcinoembryonic Antigen-Related Cell Adhesion Molecule 8); CXCL8, C-X-C Motif Chemokine Ligand 8; CD33, Cluster of Differentiation 33; BDCA-4 (NRP1), Blood Dendritic Cell Antigen 4 (Neuropilin-1); STAT1, Signal Transducer and Activator of Transcription 1; IL13, Interleukin-13; TGFB1, Transforming Growth Factor Beta 1; PD-1, Programmed Cell Death Protein 1; GZMB, Granzyme B.

and TIMER database results, the CMTM4 overexpression and CMTM4 shRNA knockdown cell lines were constructed. CMTM4 knockdown by shRNA significantly altered CD66b, CXCL8, STAT1, PD-1 and GZMB levels (Fig. 4A). However, CMTM4 overexpression did not change the mRNA level of STAT1 and GZMB (Fig. 4B). There was a negative association between CMTM4 and CD66b in the TIMER database (Table IV), but the mRNA level of CD66b was positively associated with CMTM4 in the RT-qPCR experiments (Fig. 4A and B). Therefore, CD66b has been excluded from the further analysis and CXCL8 was specifically chosen as CMTM4-regulated gene of interest. We hypothesized that CMTM4 negatively regulates CXCL8.

Next, CXCL8 expression in the surgical tissues from patients with LARC (n=56) were detected using IHC. The depth of immune cell infiltration may exhibit different functions in antitumor activity. The location of CXCL8 expression was classified into intratumor and tumor invasive margins (Fig. S3). Both the intratumor CXCL8 expression or the tumor invasive margins in the CMTM4 negative group were higher than those in the CMTM4 positive group (P=0.012 and P=0.049, respectively; Fig. 4C and D). This indicated that the location of CXCL8 did not affect the negative association between CXCL8 and CMTM4. Additionally, 5 post-nCRT tissues with high CMTM4 expression and 3 tissues with low CMTM4 expression were also collected for RT-qPCR analysis. The average relative expression of CXCL8 in the CMTM4 high group was significantly lower than the expression in the CMTM4 low group (0.075 vs. 0.646; P=0.031; Fig. S4A). The negative association between CMTM4 and CXCL8 mRNA expression was also verified. Furthermore, Kaplan-Meier (K-M) analysis results showed that CXCL8 expression in tumor margins was linked to a shorter DFS (95% CI, 1.189-6.166; P=0.018; Fig. 4E) but did not significantly affect the OS (P=0.383; Fig. 4F). There were no significant associations between CXCL8 expression in the intratumor region and survival time (DFS, P=0.546; OS, P=0.973; Fig. S4B and C). In addition, univariate analysis showed that clinicopathological characteristics such as nerve invasion, pathological tumor (pT) stage and node (N) stage indicated a poorer DFS and OS (Table V). Multivariate analysis showed that CXCL8 expression in the tumor invasive margin regions and pathological N stage were both independent DFS predictors in patients with LARC (95% CI, 1.053-10.514, P=0.041; 95% CI 1.586-10.750, P=0.004; Table VI). Therefore, CMTM4 was negatively associated with the neutrophil-related cytokine, CXCL8, in LARC tissues and CXCL8 expression in surgical tissues may be an independent prognostic factor in patients with LARC treated with nCRT.

Discussion

The CMTM family members have been shown to play important roles in different types of cancer, including CRC, clear cell renal carcinoma, HNSCC and HCC (9-11,13,14,33,34). However, CMTM4 has been much less studied compared with the other CMTM family members (8,18). Xue *et al* (9) observed lower CMTM4 expression in colorectal adenocarcinoma compared with normal tissues. The low CMTM4 expression was associated with a significantly shorter OS time based on The Human Protein Atlas database. A similar pattern was found in lung adenocarcinoma (35). CMTM4

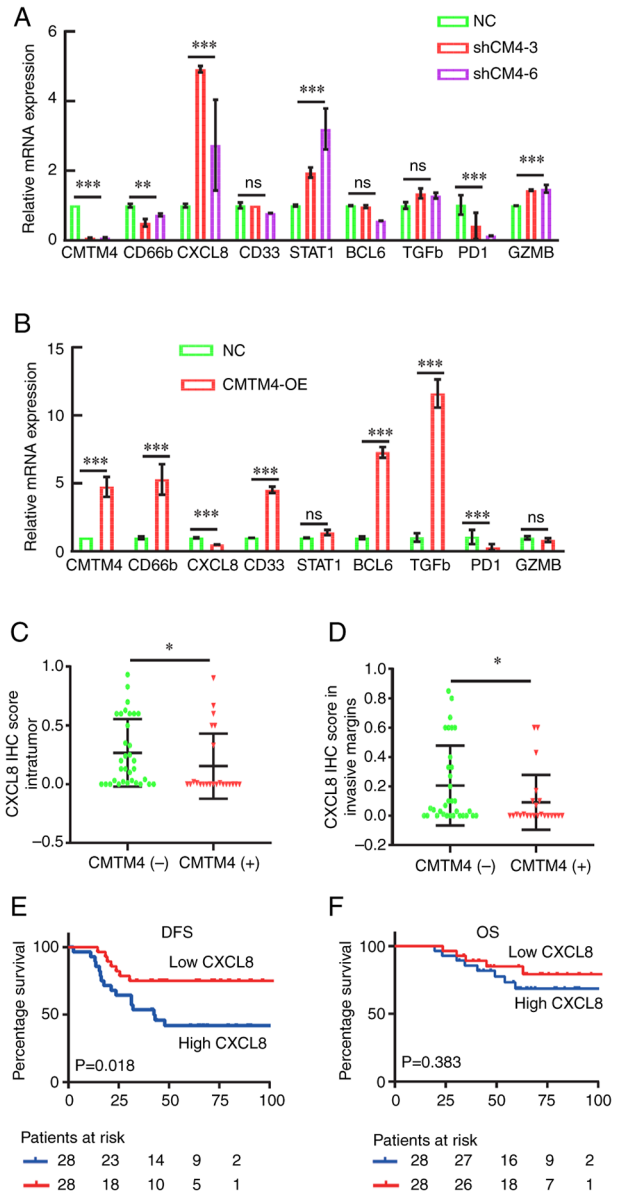

Figure 4. CXCL8 was negatively associated with CMTM4 and indicated an inferior outcome in patients with LARC. (A) RT-qPCR of RNA-seq-identified CMTM4 targets in the shCM4-3 and shCM4-6 cells, compared with NC cells. The level of GAPDH transcripts was used for normalization. (B) RT-qPCR analysis of RNA-seq-identified CMTM4 targets in the CMTM4 overexpression cells, compared with the NC cells. The level of GAPDH transcripts was used for normalization. (C) CXCL8 expression in the intratumor region was negatively correlated with CMTM4 expression in patients with LARC (n=56; P=0.012). (D) CXCL8 expression in the invasive margin region was negatively associated with CMTM4 expression in patients with LARC (n=56; P=0.049). (E) K-M analysis indicated that CXCL8 expression in tumor margins was correlated with a shorter DFS (95% CI, 1.189-6.166; P=0.018). (F) K-M analysis indicated that CXCL8 expression in tumor margins was not associated with OS in patients with LARC (P=0.383). *P<0.05, **P<0.01 and ***P<0.001. NC, negative control. CXCL8, chemokine (CXC motif) ligand 8; CMTM4, CKLF-like MARVEL transmembrane domain member 4; RT-qPCR, reverse transcription-quantitative PCR; NC, negative control; K-M, Kaplan-Meier; CI, confidence interval; DFS, disease-free survival; OS, overall survival; OE, overexpression; sh, short hairpin.

inhibited clear cell renal cell carcinoma 768-O cell-derived tumor growth in tumor xenograft model experiments (10). However, high expression of CMTM4 was found to be associated with poor prognosis in HNSCC, and interfering with CMTM4 expression inhibited EMT and expression of the cancer stem cell markers, CD44, aldehyde dehydrogenase 1, B-cell-specific Moloney murine leukemia virus integration region 1 and SRY-box 2, through the AKT pathway (11). High CMTM4 expression was also shown to be associated with poor DFS and OS in HCC by the TCGA database (12). However, CMTM4 showed no significant prognostic association with survival in patients with HCC (n=90) from Guilin Medical University (Guilin, China) (14). Therefore, the function of CMTM4 in solid tumors remains unclear, particularly the expression pattern and role of CMTM4 in rectal cancer.

The treatment of LARC has always been challenging to uncover, although new treatments such as nCRT or TNT have been established for decades. The side effects, reduced quality of life and local recurrence still cause problems in the clinic. The evaluation of clinical CR using MRI, endoscopy and digital rectal examination is suboptimal compared with the pCR following TME. The proposal of the Watch and Waite strategy also accelerated the demand to explore biomarkers to predict nCRT response in LARC before TME (36).

In the present study, the application of CMTM4 in predicting nCRT response was first explored in 228 patients with LARC, focusing on the patients with LARC (T3-4/N+M0) who received nCRT following TME. Patients with LARC and high CMTM4 expression in the biopsy tissue had a lower rate of reaching pCR status after TME (P=0.041). K-M analysis also showed that high CMTM4 expression in the biopsy tissues was associated with a lower DFS and OS. In the postoperative tissues, the expression of CMTM4 was higher in tumor tissues compared with adjacent normal tissues. No association between CMTM4 expression and survival was observed in postoperative tissues from patients with LARC (T3/T4). Considering the analysis of the published data from the TCGA database, the results indicated that the function of CMTM4 is varied in different tumor development stages or treatment stages of rectal cancer. The role of CMTM4 in treatment response has been reported in gastric cancer and HCC (12,14,34). A high percentage of CMTM4^{+} epithelial cells indicated a shorter prognosis in gastric cancer, while in mesenchymal regions, a high percentage of CMTM4^{+} cells was associated with an improved OS (34). Furthermore, CMTM4/6 exhibited higher expression in the partial response group with PDL1 therapy compared with the stable disease and progressive disease groups. Above all, radiation or immune checkpoints inhibitors therapy possibly changed the expression of CMTM4 in LARC or gastric cancer. These studies suggested the potential application of CMTM4 in nCRT or PDL1 therapy to achieve treatment response in gastrointestinal cancer.

According to the World Health Organization classification of tumors, venous invasion and perineural invasion in colorectal cancers is 4-40% and 20%, respectively (37-41). The low frequency of venous invasion and perineural invasion observed in the present study was lower than previously reported. There are two reasons for the lower frequency in the data of the present study. First, the higher the T stage, the higher the frequency of vascular and nerve invasion. A previous study enrolled 1,142 patients with CRC undergoing resection, and vascular invasion was present in 40.5% of patients with T4 rectal cancer (37). Nerve invasion in another study was present

Table V. Univariate analysis to identify prognosis-related factors in patients with LARC.

	DFS, HR (95% CI)				OS, HR (95% CI)			
Variable	P-value	HR	Lower	Upper	P-value	HR	Lower	Upper
Sex	0.833	0.905	0.356	2.297	0.741	0.802	0.217	2.965
Age	0.915	0.956	0.422	12.168	0.705	0.801	0.254	2.530
Vascular invasion	0.730	1.425	0.192	10.594	0.329	2.774	0.357	21.565
Nerve invasion	0.013	17.827	1.854	171.401	0.021	13.295	1.486	118.958
Pathological T stage	0.016	2.116	1.152	3.886	0.125	6.653	0.593	74.690
Pathological N stage	0.000	5.530	2.280	13.410	0.026	3.930	1.175	13.143
CXCL8 margins	0.023	2.797	1.150	6.803	0.253	2.013	0.606	6.691
CXCL8 intratumor	0.269	1.604	0.694	3.708	0.988	0.991	0.319	3.074

OS, overall survival; DFS, disease-free survival; HR, hazard ratio; CI, confidence interval; CXCL8, chemokine (CXC motif) ligand 8; LARC, locally advanced rectal cancer.

Table VI. Multivariate analysis to identify prognosis-related factors in patients with LARC.

	DFS, HR (95% CI)				OS, HR (95% CI)			
Variable	P-value	HR	Lower	Upper	P-value	HR	Lower	Upper
Nerve invasion	0.274	3.677	0.357	37.910	0.283	3.811	0.332	43.725
Pathological T stage	0.059	1.834	0.976	3.446	0.950	476.286	0.000	$9.16x10^{86}$
Pathological N stage	0.004	4.129	1.586	10.750	0.199	2.483	0.620	9.944
CXCL8 margins	0.041	3.328	1.053	10.514	0.299	2.075	0.524	8.219
CXCL8 intratumor	0.564	0.722	0.238	2.187	0.541	0.651	0.164	2.576

OS, overall survival; DFS, disease-free survival; HR, hazard ratio; CI, confidence interval; CXCL8, chemokine (CXC motif) ligand 8; LARC, locally advanced rectal cancer.

in 5.7% of patients with pT1-T2 and 24.0% of patients with pT3-T4 (37,38). Additionally, venous invasion and perineural invasion has not been observed in the post-operative tissues from pCR patients (41). In the present study, 55.7% of the patients were assessed as pCR, pT1 or pT2 after surgery; therefore, the observed frequency of venous invasion and perineural invasion was lower. Second, the present study was a single center retrospective study with a limited sample number. The percentage of vascular and nerve invasion in patients with LARC receiving nCRT treatment should be further proved in a multicenter large enrollment study. Additionally, the surgical team at Peking University Cancer Hospital (Beijing, China) published a study in 2018, and the lymphovascular invasion was reported as 5.4%, which is similar to the results of the present study (39).

It was confirmed in the present study that CMTM4 acted as a tumor suppressor gene in a colon cancer cell line without IR treatment, consistent with a previous study (9). Following radiation treatment, the migration and invasion ability of colon cancer cells was markedly decreased by knocking down CMTM4 expression, which agreed with the rectal cancer clinical findings. Radiation therapy has been shown to reduce the tumor size (36), while it also triggers an immune response and activates $CD8^+$ T cell infiltration (42). A positive correlation has also been found between $CD8^+$ infiltration and CMTM4 expression in the stroma region of HNSCC (11). In the context of liver cancer, CMTM4 has been shown to be the primary positive regulator of PDL1 through a post-translational mechanism (12). CMTM4/6 has been reported to stabilize PDL1 in both tumor and dendritic cells by reducing its ubiquitination. CMTM6 interacts with CD58 and PDL1. Additionally, CMTM6 depletion activates the tumor specific perforin- and TNFα producing $CD8^+$ T cell activity through PDL1 (16,17,33). In the present study, to examine the downstream genes of CMTM4, RNA-seq and TIMER database analyses were performed. Colon cancer cells were used in the present study as the knockdown of CMTM4 expression was more notable in LoVo cells than the rectal cell lines, such as SW480 (data not shown). The expression levels of 105 genes were changed after knocking down CMTM4 expression in the LoVo cells. CXCL8 was the only gene negatively associated with CMTM4 expression in both the RNA-seq and TIMER analyses. The negative association was confirmed by RT-qPCR and IHC staining. The expression levels of CXCL8 and CMTM4 were detected in tissues from patients with LARC to confirm the results obtained from the colon cancer cell line.

CXCL8, a proinflammatory chemokine, is expressed in epithelial and macrophage cells and recruits neutrophils

to inflammatory sites (43). CXCL8 is induced by immune infiltration cells, stromal cells and tumor cells in the tumor microenvironment (44,45). Multiple G protein-mediated signaling pathway cascades are activated by CXCL8-CXCR1/2 binding, including the PI3K-Akt, ERK-MAPK, P38-MAPK, FAK-Src and JAK-STAT pathways (46-52). CXCL8 participates in tumor cell motility, angiogenesis and survival through these signaling pathways. The expression level of CXCL8 serves as a prognostic marker in numerous types of cancer. For instance, the stroma level of CXCL8 was shown to be negatively associated with the 5-year survival rate in right-side colon cancer (53), which was consistent with the results of the present study. High expression of CXCL8 was also shown to indicate poor prognosis in triple-negative and estrogen receptor-negative breast cancer (54,55). CXCL8 expression is also positively correlated with lymph node metastasis and TNM stage in patients with non-small cell lung cancer (56). CXCL8 secreted by tumors through paracrine signaling recruits neutrophils and macrophages into the tumor microenvironment and inhibits the antitumor immune activity (57). Thus, CXCL8 is associated with chemotherapy and immunotherapy resistance in breast, gastric, prostate and pancreatic cancer (58-62). In the present study, the prognostic role of CXCL8 was reported in patients with LARC subjected to nCRT. CXCL8 expression was negatively associated with CMTM4 expression in postoperative tissues and CXCL8 expression indicated a shorter DFS time, but not OS time. The role of CXCL8 in the prediction of nCRT response in pre-operative tissues was not investigated in the present study. This is because the role of CXCL8 in radiotherapy or chemoradiotherapy is unclear, particularly in rectal cancer. In head and neck cancer, lower salivary CXCL8 levels indicate improved radiotherapy outcomes (63). Additionally, higher CXCL8 expression in head and neck squamous carcinoma tissues is associated with a lower 5-year local recurrence-free survival (64). In the present study, CMTM4, which indicated an unfavorable nCRT response and DFS, was not associated with DFS and OS in postoperative tissues. Therefore, CXCL8 combined CMTM4 may predict outcomes in patients with LARC on two independent time points: Biopsy tissues from pre-nCRT and surgery tissues.

In conclusion, CMTM4 may be a new nCRT response prediction biomarker in patients with LARC. CMTM4 may serve as a target to sensitize chemoradiation therapy in patients with LARC. In the present study, high CXCL8 expression indicated poorer outcomes in patients with LARC who received TME followed by nCRT.

Acknowledgements

The authors would like to thank Miss Jiayi Ma (Beijing National Day School, Beijing 100039, P.R. China) for experimental assistance including cell culture, migration and invasion.

Funding

This work was supported by PKU-Baidu Fund (grant no. A002292), the Capital's Funds for Health Improvement and Research (grant no. 2022-2-1024), Peking University Medicine Seed Fund for Interdisciplinary Research (grant no. BUM2020MX009), the Capital's Funds for Health Improvement and Research (grant no. 2018-2-1022), the Beijing Municipal Science and Technology Commission Capital Characteristic Clinical Application Research (grant no. Z141107002514077), the National Natural Science Foundation of China (grant no. 81872309) and the National Natural Science Foundation of China (grant no. 61501039).

Availability of data and materials

The RNA-sequencing data generated in the present study may be found in the Sequence Read Archive under accession no. PRJNA1176295 or at the following URL: https://www.ncbi.nlm.nih.gov/bioproject/PRJNA1176295. All other data generated in the present study may be requested from the corresponding author.

Authors' contributions

ZWL and SYL contributed to the study conception and design. LJY, ZTM, NNL and SYL wrote the first draft of the manuscript. LJY, ZTM, NNL and YHB were responsible for collecting the patient's information and the IHC investigation and assessment. ZTM, LM, QF, DBQ, YW and PW were responsible for material preparation, data collection and analysis. LJY, YHB, ZWL and SYL provided comments on previous versions of the manuscript. ZWL and SYL confirm the authenticity of all the raw data. All authors read and approved the final version of the manuscript.

Ethics approval and consent to participate

The present study was approved by the Ethics Committee of Peking University Cancer Hospital & Institute (Beijing, China; approval no. 2021KT93).

Patient consent for publication

Not applicable.

Competing interests

The authors declare that they have no competing interests.

References

1. Sung H, Ferlay J, Siegel RL, Laversanne M, Soerjomataram I, Jemal A and Bray F: Global cancer statistics 2020: GLOBOCAN estimates of incidence and mortality worldwide for 36 cancers in 185 countries. CA Cancer J Clin 71: 209-249, 2021.
2. Xia C, Dong X, Li H, Cao M, Sun D, He S, Yang F, Yan X, Zhang S, Li N and Chen W: Cancer statistics in China and United States, 2022: Profiles, trends, and determinants. Chin Med J (Engl) 135: 584-590, 2022.
3. Dekker E, Tanis PJ, Vleugels JLA, Kasi PM and Wallace MB: Colorectal cancer. Lancet 394: 1467-1480, 2019.
4. Wang Y, Shen L, Wan J, Zhang H, Wu R, Wang J, Wang Y, Xu Y, Cai S, Zhang Z and Xia F: Neoadjuvant chemoradiotherapy combined with immunotherapy for locally advanced rectal cancer: A new era for anal preservation. Front Immunol 13: 1067036, 2022.
5. Mei WJ, Wang XZ, Li YF, Sun YM, Yang CK, Lin JZ, Wu ZG, Zhang R, Wang W, Li Y, *et al*: Neoadjuvant chemotherapy with CAPOX versus chemoradiation for locally advanced rectal cancer with uninvolved mesorectal fascia (CONVERT): Initial results of a phase III trial. Ann Surg 277: 557-564, 2023..

6. Peeters KCMJ, Marijnen CAM, Nagtegaal ID, Kranenbarg EK, Putter H, Wiggers T, Rutten H, Pahlman L, Glimelius B, Leer JW, *et al*: The TME trial after a median follow-up of 6 years: Increased local control but no survival benefit in irradiated patients with resectable rectal carcinoma. Ann Surg 246: 693-701, 2007.
7. Kapiteijn E, Marijnen CA, Nagtegaal ID, Putter H, Steup WH, Wiggers T, Rutten HJ, Pahlman L, Glimelius B, van Krieken JH, *et al*: Preoperative radiotherapy combined with total mesorectal excision for resectable rectal cancer. N Engl J Med 345: 638-646, 2001.
8. Wu J, Li L, Wu S and Xu B: CMTM family proteins 1-8: Roles in cancer biological processes and potential clinical value. Cancer Biol Med 17: 528-542, 2020.
9. Xue H, Li T, Wang P, Mo X, Zhang H, Ding S, Ma D, Lv W, Zhang J and Han W: CMTM4 inhibits cell proliferation and migration via AKT, ERK1/2, and STAT3 pathway in colorectal cancer. Acta Biochim Biophys Sin (Shanghai) 51: 915-924, 2019
10. Li T, Cheng Y, Wang P, Wang W, Hu F, Mo X, Lv H, Xu T and Han W: CMTM4 is frequently downregulated and functions as a tumour suppressor in clear cell renal cell carcinoma. J Exp Clin Cancer Res 34: 122, 2015.
11. Li H, Liu YT, Chen L, Zhou JJ, Chen DR, Li SJ and Sun ZJ: CMTM4 regulates epithelial-mesenchymal transition and PD-L1 expression in head and neck squamous cell carcinoma. Mol Carcinog 60: 556-566, 2021.
12. Chui NN, Cheu JW, Yuen VW, Chiu DK, Goh CC, Lee D, Zhang MS, Ng IO and Wong CC: Inhibition of CMTM4 sensitizes cholangiocarcinoma and hepatocellular carcinoma to T cell-mediated antitumor immunity through PD-L1. Hepatol Commun 6: 178-193, 2022.
13. Zhou HQ, Li JH, Liu LW, Lou JM and Ren ZG: Increased CMTM4 mRNA expression predicts a poor prognosis in patients with hepatocellular carcinoma. Hepatobiliary Pancreat Dis Int 19: 596-601, 2020.
14. Tan S, Guo X, Bei C, Zhang H, Li D, Zhu X and Tan H: Prognostic significance and immune characteristics of CMTM4 in hepatocellular carcinoma. BMC Cancer 22: 905, 2022.
15. Bei C, Zhang Y, Wei R, Zhu X, Wang Z, Zeng W, Chen Q and Tan S: Clinical significance of CMTM4 expression in hepatocellular carcinoma. Onco Targets Ther 10: 5439-5443, 2017.
16. Mezzadra R, Sun C, Jae LT, Gomez-Eerland R, de Vries E, Wu W, Logtenberg MEW, Slagter M, Rozeman EA, Hofland I, *et al*: Identification of CMTM6 and CMTM4 as PD-L1 protein regulators. Nature 549: 106-110, 2017.
17. Burr ML, Sparbier CE, Chan YC, Williamson JC, Woods K, Beavis PA, Lam EYN, Henderson MA, Bell CC, Stolzenburg S, *et al*: CMTM6 maintains the expression of PD-L1 and regulates anti-tumour immunity. Nature 549: 101-105, 2017.
18. Zhang T, Yu H, Dai X and Zhang X: CMTM6 and CMTM4 as two novel regulators of PD-L1 modulate the tumor microenvironment. Front Immunol 13: 971428, 2022.
19. Wang L, Li ZY, Li ZW, Li YH, Sun YS, Ji JF, Gu J and Cai Y: Efficacy and safety of neoadjuvant intensity-modulated radiotherapy with concurrent capecitabine for locally advanced rectal cancer. Dis Colon Rectum 58: 186-192, 2015.
20. Cuccurullo V and Mansi L: AJCC cancer staging handbook: From the AJCC Cancer Staging Manual (7th edition). Eur J Nucl Med Mol Imaging 38: 408, 2011.
21. Wen Z, Luo D, Wang S, Rong R, Evers BM, Jia L, Fang Y, Daoud EV, Yang S, Gu Z, *et al*: Deep learning-based h-score quantification of immunohistochemistry-stained images. Mod Pathol 37: 100398, 2024.
22. Matos LL, Trufelli DC, de Matos MG and da Silva Pinhal MA: Immunohistochemistry as an important tool in biomarkers detection and clinical practice. Biomark Insights 5: 9-20, 2010.
23. Li T, Fan J, Wang B, Traugh N, Chen Q, Liu JS, Li B and Liu XS: TIMER: A web server for comprehensive analysis of tumor-infiltrating immune cells. Cancer Res 77: e108-e110, 2017.
24. Danaher P, Warren S, Dennis L, D'Amico L, White A, Disis ML, Geller MA, Odunsi K, Beechem J and Fling SP: Gene expression markers of tumor infiltrating leukocytes. J Immunother Cancer 5: 18, 2017.
25. Ginestet C: ggplot2: Elegant graphics for data analysis. Journal of the Royal Statistical Society Series A: Stat Soc 174: 245-246, 2011.
26. Subramanian A, Tamayo P, Mootha VK, Mukherjee S, Ebert BL, Gillette MA, Paulovich A, Pomeroy SL, Golub TR, Lander ES and Mesirov JP: Gene set enrichment analysis: A knowledge-based approach for interpreting genome-wide expression profiles. Proc Natl Acad Sci USA 102: 15545-15550, 2005.
27. Huang DW, Sherman BT and Lempicki RA: Bioinformatics enrichment tools: Paths toward the comprehensive functional analysis of large gene lists. Nucleic Acids Res 37: 1-13, 2009.
28. Huang DW, Sherman BT and Lempicki RA: Systematic and integrative analysis of large gene lists using DAVID bioinformatics resources. Nat Protoc 4: 44-57, 2009.
29. Livak KJ and Schmittgen TD: Analysis of relative gene expression data using real-time quantitative PCR and the 2(-Delta Delta C(T)) method. Methods 25: 402-408, 2001.
30. Martin ST, Heneghan HM and Winter DC: Systematic review and meta-analysis of outcomes following pathological complete response to neoadjuvant chemoradiotherapy for rectal cancer. Br J Surg 99: 918-928, 2012.
31. Wen J, Fang S, Hu Y, Xi M, Weng Z, Pan C, Luo K, Ling Y, Lai R, Xie X, *et al*: Impacts of neoadjuvant chemoradiotherapy on the immune landscape of esophageal squamous cell carcinoma. EBioMedicine 86: 104371, 2022.
32. Shi M, Chen Y and Ji D: The implications from the interplay of neoadjuvant chemoradiotherapy and the immune microenvironment in rectal cancer. Future Oncol 18: 3229-3244, 2022.
33. Miao B, Hu Z, Mezzadra R, Hoeijmakers L, Fauster A, Du S, Yang Z, Sator-Schmitt M, Engel H, Li X, *et al*: CMTM6 shapes antitumor T cell response through modulating protein expression of CD58 and PD-L1. Cancer Cell 41: 1817-1828.e1819, 2023.
34. Wang Z, Peng Z, Liu Q, Guo Z, Menatola M, Su J, Li T, Ge Q, Wang P, Shen L and Jin R: Co-expression with membrane CMTM6/4 on tumor epithelium enhances the prediction value of PD-L1 on Anti-PD-1/L1 therapeutic efficacy in gastric adenocarcinoma. Cancers (Basel) 13: 5175, 2021.
35. Zhu X, Zhang S, Tan S, Li D, Chen X, Kong J, Fu Y, Wang C and Wen L: Expression of CMTM4 shows clinical significance in lung cancer. Transl Cancer Res 9: 6214-6220, 2020.
36. Liu S, Jiang T, Xiao L, Yang S, Liu Q, Gao Y, Chen G and Xiao W: Total neoadjuvant therapy (TNT) versus standard neoadjuvant chemoradiotherapy for locally advanced rectal cancer: A systematic review and meta-analysis. Oncologist 26: e1555-e1566, 2021.
37. Bhangu A, Fitzgerald JE, Slesser A, Northover JM, Faiz O and Tekkis P: Prognostic significance of extramural vascular invasion in T4 rectal cancer. Colorectal Dis 15: e665-e671, 2013.
38. Chablani P, Nguyen P, Pan X, Robinson A, Walston S, Wu C, Frankel WL, Chen W, Bekaii-Saab T, Chakravarti A, *et al*: Perineural invasion predicts for distant metastasis in locally advanced rectal cancer treated with neoadjuvant chemoradiation and surgery. Am J Clin Oncol 40: 561-568, 2017.
39. Wu AW, Cai Y, Li YH, Wang L, Li ZW, Sun YS and Ji JF: Pattern and management of recurrence of mid-low rectal cancer after neoadjuvant intensity-modulated radiotherapy: Single-center results of 687 cases. Clin Colorectal Cancer 17: e307-e313, 2018.
40. Liu S, Yang S, Yu H, Luo H, Chen G, Gao Y, Sun R and Xiao W: A nomogram for predicting 10-year cancer specific survival in patients with pathological T3N0M0 rectal cancer. Front Med (Lausanne) 9: 977652, 2022.
41. Shin JK, Huh JW, Lee WY, Yun SH, Kim HC, Cho YB and Park YA: Clinical prediction model of pathological response following neoadjuvant chemoradiotherapy for rectal cancer. Sci Rep 12: 7145, 2022.
42. Sinha UK, Kast WM and Lin DC: Single-cell genomics identifies immune response to neoadjuvant chemoradiotherapy. EBioMed 86: 104389, 2022.
43. Holmes WE, Lee J, Kuang WJ, Rice GC and Wood WI: Structure and functional expression of a human interleukin-8 receptor. Science 253: 1278-1280, 1991.
44. Waugh DJ and Wilson C: The interleukin-8 pathway in cancer. Clin Cancer Res 14: 6735-6741, 2008.
45. Alfaro C, Sanmamed MF, Rodríguez-Ruiz ME, Teijeira Á, Oñate C, González Á, Ponz M, Schalper KA, Pérez-Gracia JL and Melero I: Interleukin-8 in cancer pathogenesis, treatment and follow-up. Cancer Treat Rev 60: 24-31, 2017.
46. Meng ZW, Zhang L, Cai XR, Wang X, She FF and Chen YL: IL-8 is a novel prometastatic chemokine in intrahepatic cholangiocarcinoma that induces CXCR2-PI3K/AKT signaling upon CD97 activation. Sci Rep 13: 18711, 2023.
47. Chen F, Aye L, Yu L, Liu L, Liu Y, Lin Y, Gao D, Gao Q and Zhang S: SSH1 promotes progression of intrahepatic cholangiocarcinoma via p38 MAPK-CXCL8 axis. Carcinogenesis 44: 232-241, 2023.
48. Zhang SQ, Wang LL, Li YT, Wang G, Li L, Sun SZ, Yao LJ and Shen L: MicroRNA-126 attenuates the effect of chemokine CXCL8 on proliferation, migration, apoptosis, and MAPK-dependent signaling activity of vascular endothelial cells cultured in a medium with high glucose concentration. Bull Exp Biol Med 171: 202-207, 2021.

49. Petreaca ML, Yao M, Liu Y, Defea K and Martins-Green M: Transactivation of vascular endothelial growth factor receptor-2 by interleukin-8 (IL-8/CXCL8) is required for IL-8/CXCL8-induced endothelial permeability. Mol Biol Cell 18: 5014-5023, 2007.
50. Ahmed S, Mohamed HT, El-Husseiny N, El Mahdy MM, Safwat G, Diab AA, El-Sherif AA, El-Shinawi M and Mohamed MM: IL-8 secreted by tumor associated macrophages contribute to lapatinib resistance in HER2-positive locally advanced breast cancer via activation of Src/STAT3/ERK1/2-mediated EGFR signaling. Biochim Biophys Acta Mol Cell Res 1868: 118995, 2021.
51. Fu XT, Dai Z, Song K, Zhang ZJ, Zhou ZJ, Zhou SL, Zhao YM, Xiao YS, Sun QM, Ding ZB and Fan J: Macrophage-secreted IL-8 induces epithelial-mesenchymal transition in hepatocellular carcinoma cells by activating the JAK2/STAT3/Snail pathway. Int J Oncol 46: 587-596, 2015.
52. Hu X, Yuan L and Ma T: Mechanisms of JAK-STAT signaling pathway mediated by CXCL8 gene silencing on epithelial-mesenchymal transition of human cutaneous melanoma cells. Oncol Lett 20: 1973-1981, 2020.
53. Pennel KA, Quinn JA, Nixon C, Inthagard J, van Wyk HC, Chang D, Rebus S; GPOL Group; Hay J, Maka NN, *et al*: CXCL8 expression is associated with advanced stage, right sided ness, and distinct histological features of colorectal cancer. J Pathol Clin Res 8: 509-520, 2022.
54. Shen Y, Zhang B, Wei X, Guan X and Zhang W: CXCL8 is a prognostic biomarker and correlated with TNBC brain metastasis and immune infiltration. Int Immunopharmacol 103: 108454, 2022.
55. Fang QI, Wang X, Luo G, Yu M, Zhang X and Xu N: Increased CXCL8 expression is negatively correlated with the overall survival of patients with er-negative breast cancer. Anticancer Res 37: 4845-4852, 2017.
56. Gu L, Yao Y and Chen Z: An inter-correlation among chemokine (C-X-C motif) ligand (CXCL) 1, CXCL2 and CXCL8, and their diversified potential as biomarkers for tumor features and survival profiles in non-small cell lung cancer patients. Transl Cancer Res 10: 748-758, 2021.
57. David JM, Dominguez C, Hamilton DH and Palena C: The IL-8/IL-8R axis: A double agent in tumor immune resistance. Vaccines (Basel) 4: 22, 2016.
58. Zhang M, Huang L, Ding G, Huang H, Cao G, Sun X, Lou N, Wei Q, Shen T, Xu X, *et al*: Interferon gamma inhibits CXCL8-CXCR2 axis mediated tumor-associated macrophages tumor trafficking and enhances anti-PD1 efficacy in pancreatic cancer. J Immunother Cancer 8: e000308, 2020.
59. Yi M, Peng C, Xia B and Gan L: CXCL8 facilitates the survival and paclitaxel-resistance of triple-negative breast cancers. Clin Breast Cancer 22: e191-e198, 2022.
60. Wang RX, Ji P, Gong Y, Shao ZM and Chen S: Value of CXCL8-CXCR1/2 axis in neoadjuvant chemotherapy for triple-negative breast cancer patients: A retrospective pilot study. Breast Cancer Res Treat 181: 561-570, 2020.
61. Wilson C, Purcell C, Seaton A, Oladipo O, Maxwell PJ, O'Sullivan JM, Wilson RH, Johnston PG and Waugh DJ: Chemotherapy-induced CXC-chemokine/CXC-chemokine receptor signaling in metastatic prostate cancer cells confers resistance to oxaliplatin through potentiation of nuclear factor-kappaB transcription and evasion of apoptosis. J Pharmacol Exp Ther 327: 746-759, 2008.
62. Lin C, He H, Liu H, Li R, Chen Y, Qi Y, Jiang Q, Chen L, Zhang P, Zhang H, *et al*: Tumour-associated macrophages-derived CXCL8 determines immune evasion through autonomous PD-L1 expression in gastric cancer. Gut 68: 1764-1773, 2019.
63. Principe S, Zapater-Latorre E, Arribas L, Garcia-Miragall E and Bagan J: Salivary IL-8 as a putative predictive biomarker of radiotherapy response in head and neck cancer patients. Clin Oral Investig 26: 437-448, 2022.
64. León X, García J, Farré N, Majercakova K, Avilés-Jurado FX, Quer M and Camacho M: Predictive capacity of IL-8 expression in head and neck squamous carcinoma patients treated with radiotherapy or chemoradiotherapy. Acta Otorrinolaringol Esp (Engl Ed) 72: 337-343, 2021.